Is terahertz emission a good probe of the spin current attenuation length?

Jon Gorchon, Stéphane Mangin, Michel Hehn, Gregory Malinowski

Is terahertz emission a good probe of the spin current attenuation length?

Jon Gorchon[1,*], Stéphane Mangin[1], Michel Hehn[1], Gregory Malinowski[1,*]

[1]Université de Lorraine, CNRS, IJL, F-54000 Nancy, France

*Authors to whom correspondence should be addressed:

Jon Gorchon, jon.gorchon@univ-lorraine.fr; Gregory Malinowki, gregory.malinowski@univ-lorraine.fr

Terahertz (THz) emission from magnetic films has recently become an important characterization tool of spintronic properties, particularly since no patterning is required. One such property of interest is the spin-current attenuation length. When separating a magnetic film from a spin-to-charge converter with a light metal, the emitted intensity reduces almost exponentially with the thickness of the spacer. However, the extracted characteristic length is more than an order of magnitude smaller than the spin diffusion length measured in equilibrium. In this work, we experimentally and theoretically demonstrate that most of the observed decay in the THz emission is of optical (THz) origin. We are able to estimate a spin current attenuation length for Cu of ~50 nm in much closer agreement with spin diffusion length measurements. We conclude that THz emission remains a powerful characterization technique, but due to the high number of intricate conversion mechanisms, and most importantly, due to the high sensitivity to changes in the optical properties, extracting absolute numbers for spintronic phenomena remains extremely challenging.

Ultrafast spin polarized currents triggered by laser pulses excitation in magnetic heterostructures present a fascinating opportunity for studying, controlling and using spintronics phenomena on the femtosecond timescale. Following the laser pulse absorption, hot carriers are created which propagate at high velocities over distances of few tens of nanometer. In ferromagnetic materials, the excitation results in the creation of a spin-polarized current. Moreover, very high spin-polarization can be achieved due to the spin-filtering effect since the lifetime and velocities of excited carriers are spin-dependent and significantly higher for majority spins compared to minority spins [1]. This spin current can therefore propagate into other layers within a metallic multilayer [2–4]. When injected into another ferromagnetic layer, it has been shown to modify the ultrafast demagnetization amplitude and characteristic time [5], to trigger magnetization precession due to ultrafast spin-transfer torque [4,6–8] and even to induce magnetization switching in magnetic spin-valve structures [9–11].

More recently, this ultrafast spin current has been used to develop spintronic THz emitters [12–16]. These emitters usually consist of a ferromagnetic (FM) / heavy metal (HM) bilayer. The optically generated spin current in the FM is injected into the HM and converted into a charge current due to the inverse spin Hall effect [17] (or other spin-to-charge conversion effects), finally resulting in the emission of a THz pulse. From an application point of view, these THz radiation sources have already proven to outperform standard THz sources in terms of bandwidth, simplicity of fabrication, tunability... From a fundamental point of view, they offer the possibility to study ultrafast spin dynamics and spin transport in metallic multilayers through time domain spectroscopy. Indeed, the measure of the THz signal is regularly used to compare or extract a number of spintronic relevant parameter, such as spin-to-charge conversion efficiencies [14,18,19], spin-transparencies [20] and spin current attenuation lengths [14,15,18]. Particularly, a number of groups have shown that the amplitude of the THz emission drops drastically when a light-metal spacer is added between the magnetic layer and the spin-to-charge converter [15,18,21], which is often attributed to changes in the spin-transport. For example, by comparing the THz emission with varying spacer thicknesses, a spin current attenuation length in Cu has been estimated [15,18] to 1.3-11 nm. Surprisingly, transport experiments yield generally much larger numbers for spin diffusion lengths, around > 100 nm for Cu at room temperature [22]. This discrepancy could be attributed to the high-energy or strongly out-of-equilibrium character of electrons found during ultrafast optical excitations which are in strong contrast to the near-equilibrium electrons probed during transport measurements [15,23] (in the following, we will use the term spin current attenuation length to explicitly take into account the out-of-equilibrium nature of photoexcited electrons). The same argument was brought forward by Schellekens et al. after reporting spin current attenuation lengths of 13nm [6]. However, high-energy electrons are not necessarily involved in ultrafast demagnetization and spin-current generation [4,24,25]. Moreover, Choi *et al.* observed ultrafast spin transport across 120 nm of Cu using a picosecond-wide laser excitation [4], which would have been impossible to detect with sub-10 nm attenuation lengths. Finally, the electron lifetime in Cu

has been measured by different groups as a function of their energy using time-resolved two photons photoemission (see Ref. [26] and reference therein). Assuming an electron lifetime of 25 fs at 1.5 eV and a velocity similar to the Fermi velocity in Cu ($1.5x10^6$ m/s), the electron mean free math should be larger than 35 nm. This gives a low limit for the spin current attenuation length which is much larger than some of the reported values. Therefore, the importance of the electron energy distribution and its spin transport properties in the THz emission process still remains an open question.

In this letter, we compare the influence of a Cu layer on the emitted THz amplitude when its placed between the FM and HM versus when its placed on top of the FM/HM bilayer. We show that increasing the inserted Cu layer results in a strong attenuation of the amplitude of the emitted THz, regardless of its position, which demonstrates that spin-transport alone cannot be responsible for the drop in signal. Simulations based on the transfer-matrix method allows us to conclude that this attenuation is overwhelmingly dominated by the reduction in the radiation efficiency of the stack. Therefore, we believe that THz emission measurements are not ideally suited for the evaluation of spin diffusion length of excited carriers unless the strongly dominant THz optical response of the whole system can be perfectly taken into account.

Two types of samples have been grown by DC magnetron sputtering with the following structure Glass/Ta(3 nm)/Co(2 nm)/ Pt(2.3 nm)/ Cu(t nm)/Al(3 nm) and Glass/Ta(3 nm)/Co(2 nm)/Cu(t nm)/Pt(2.3 nm) with t = 1, 2, 4, 8, 16 nm. The Al (3 nm) is used to protect the Cu layer from oxidizing and it is passivated forming an AlOx layer. The main difference between both types of samples resides in the positioning of the Cu layer: either on top of the Co/Pt bilayer, or in between the Pt and Co layers. The spin currents are generated within the Co layer during ultrafast demagnetization, and propagate (mostly) perpendicular to the plane of the samples, into the Pt or Cu layers.

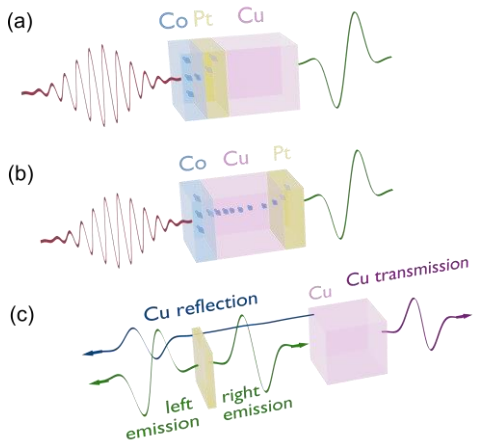

Figure 1: Experimental schematic: Samples are pumped with an IR pulse (red), and the THz (green) emitted on the opposite side are detected. Structures with Cu on top of the spintronic emitter (a) or Cu as a spacer (b) are studied. (c) Schematic of the reduction in THz emission of a source (yellow plane) placed near a Cu "mirror". Destructive interference (left) and reduced transmission (right) result in a reduced THz detection in both directions.

To perform the THz TDS measurement, we used a Ti:Sa regenerative amplifier with a central wavelength of 800 nm, a pulse duration of 35 fs and a repetition rate of 5 KHz. The laser beam was split in two parts, a large (roughly 1 mm FWHM) pump beam impinging on the sample at normal incidence is used to excite the magnetic multilayer and a probe beam which is used to detect the THz pulse via electro-optic sampling in a 1 mm thick <110> ZnTe crystal [27,28]. The pump power was kept constant for all the reported measurements which were carried at room temperature. An external Nd-based permanent magnet was used to ensure a full saturation of the in plane Co magnetization (THz signals were confirmed to be symmetric with magnetic field [13]). We excited the samples either from the metal side or through the glass substrate while we analyzed the emitted THz wave on the opposite side.

The detected THz traces are shown in **Figure *2***. We first remark that when exciting the samples through the substrate (**Figure *2***.a) both type of samples emit extremely similar THz waves for equal Cu thicknesses. Moreover, both types of samples show a strong attenuation of the emitted THz when increasing the Cu thicknesses. When exciting the Co/Pt/Cu series from the top metal side (**Figure *2***.b) a smaller THz amplitude and a broader temporal profile are detected, most likely due to dispersion and absorption of the THz in the substrate. Interestingly, we find here also a similar attenuation of the THz emission with the Cu thickness.

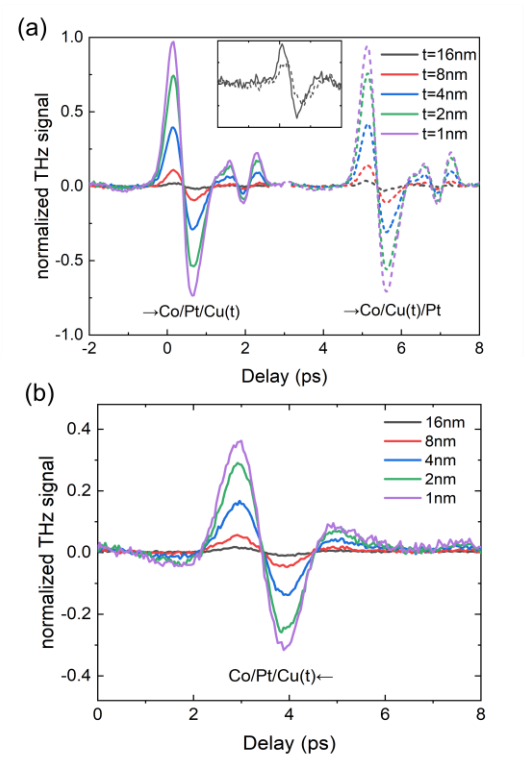

Figure 2: Detected THz signal for the Co/Pt/Cu(t) (solid line) and Co/Cu(t)/Pt (dashed line) samples of various thicknesses (t). (a) Samples where excited a) through the glass substrate and (b) from the metal side. All data has been normalized by the peak signal of the Pt/Co/Cu(t=1 nm) sample excited through the susbtrate. The time-delay for the Co/Cu(t)/Pt series has been shifted by +5 ps for comparison. The inset zooms into the t=16 nm signals to highlight the small emission differences between the two type of samples.

In order to explain our experimental results, we first calculated the total absorption of the 800 nm excitation pulse within our multilayer as a function of the Cu thickness [18]. While the absorption is changing when increasing the Cu thickness, it only varies by a factor of 2 at most and cannot explain the differences measured in the emitted THz pulse amplitude [18]. According to Seifert et al. [18], the THz emission is proportional to the total absorption divided by the total thickness, but is also dependent on the impedance of the film and on the hot electron spin relaxation length (the equivalent of the spin diffusion length but for high-energy ballistic electrons). However, for two films with same thickness and effective impedance (same materials, same conductivities), only the differences in total optical absorption and spin transport should play a role. We therefore simply plot the ratio of peak signals between the two families of samples, for each thickness of Cu, multiplied by the ratio of total optical absorptions (see **Figure 3**). This final ratio should highlight only spin transport related variations. We then try to fit a single exponential decay function with a characteristic spin current attenuation length (λ) of 50 nm (solid line) and 5 nm (dashed line).

We can clearly see that to account for the small changes in the ratio, a rather long spin-current attenuation length on the order of 50 nm needs to be assumed. As predicted by Yang et al. [29], we believe that most estimations in the literature might under-estimate the spin-current attenuation length if they do not properly account for the largely dominant contribution to the signal attenuation from the THz optics. In the following we will attempt to give a more intuitive understanding of the complexity of the problem and will develop a model to account for the sharp drop in THz signal.

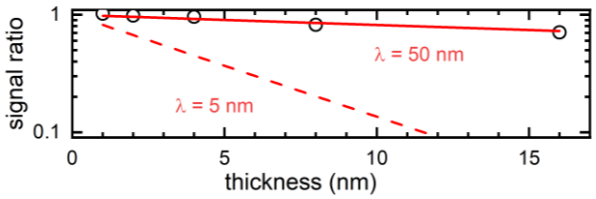

Figure 3: Ratio of the peak signal in Co/Cu(t)/Pt over the peak signal in Co/Pt/Cu(t) as a function of Cu thickness. The ratio is multiplied by the ratio of total absorptions A_{CoPtCu}/A_{CoCuPt}. Lines are single exponential decay fits with λ = 50 nm (solid) and λ = 5 nm (dashed).

The THz source in spintronic emitters is located inside the stack, which, surrounded by air and glass, acts as an optical cavity [13]. This is a very different scenario from that of an incident THz. In the following we highlight a few phenomena taking place within the film: As already pointed out by Seifert et al. [13], when the metal meets the air or glass interface, the index of refraction is typically drastically reduced, inducing a phase-maintaining reflection which constructively interferes and enhances the THz electric field inside the cavity. However, there exists an opposite effect too. Inside the metal stack, when the wave meets a higher-index material (usually a better conductor), a 180-degree phase shifted reflection occurs, which results in a decreased electric field. Even in the case of a single Cu interface next to the current source such as shown in **Figure *1***.c, both the right and left propagating THz waves will have an amplitude of 1-R where R is the interface reflectivity (assuming no absorption in Cu). The latter effect can also be understood as a shunting effect, where the nearby high-conductivity metal screens the spin-to-charge driven E field surge of the source [13,19]. These cavity optimizations to enhance the emission of an embedded source are sometimes known as the Purcell effect [30–34], and are governed by the Purcell factor. Ultimately, as stated by Seifert et al. [13], index (i.e. impedance) matching the emitter to air (i.e. having a lower effective conductivity in the stack) and reducing the thickness to confine the field should result in a higher emission.

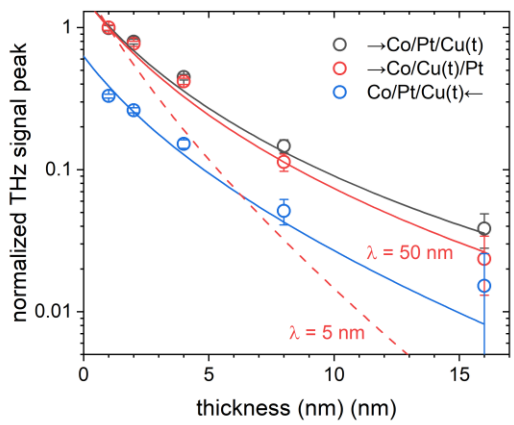

Figure 4: Peak of the normalized THz signal as a function of Cu thickness (t). Circles represent the data points extracted from **Figure *2*** whereas lines are fits using the transfer matrix model (see text). The red solid line assumes a λ = 50 nm whereas the dashed line uses λ = 5 nm.

In order to gain more insights into the emission process, we developed a model [35] based on the transfer-matrix approach in which we consider a THz current source [29,36,37] located at the interface of the Pt layer nearest to the Co. To this aim we assume an infinitely thin slab of current oscillating at THz frequencies which creates a discontinuity in the tangential H field within the stack. We then calculate the total electromagnetic field inside and outside the film ($\mathrm{E_{TTM}}$) by setting the incident waves to zero. Optical indices are selected at 1THz (our data's FFT peaks at 1THz) as follows,

Glass [38,39]	Ta/Co	Pt [40]	Cu [41,42]	Al_2O_3 [39]
2	270+400i	80+60i	270+511i	3.31

Table 1: THz optical indices used in the transfer matrix model. The Ta/Co index is used as a fit parameter.

The influence on the spin transport of the intercalated Cu layer was included as an exponential decay of the generated THz emission characterized by the spin-current attenuation length of Cu. We also include an additional factor to consider the absorption of the laser by the Co layer A_{Co} which determines the amount of spin current generation. We note here that other works [13,18,20] assume instead that the spin current is proportional to the total absorption divided by the total thickness. Such assumption implies that all the absorbed energy is redistributed instantly within all the thickness of the stack, and that it is the resulting energy density within the magnet that drives the spin current. However, such an assumption goes against any ballistic spin transport scenario, since such a redistribution of energy would require electronic thermalization, and therefore transport should then be purely diffusive. Moreover, since the thermalization process itself is a major contributor to the spin current generation we believe that this hypothesis might lead to an under-estimation of the spin currents for thick metal films. In fact, it has been shown that the peak demagnetization (and the resulting spin current injection) does not strongly depend on the thickness of the Cu heat sink below the ferromagnet [4]. Our model outputs a THz intensity given by,

$$I_{THz} = A_{Co} e^{-\left(\frac{t}{\lambda}\right)} \cdot \mathrm{E_{TTM}} \mathrm{E_{TTM}^{*}}$$

In **Figure 4** we show the peak THz fields as a function of the Cu thickness extracted from the experimental data in **Figure *2***. We also show fits using our model, assuming both a 5 and a 50 nm spin-current attenuation length in Cu (dashed and solid lines respectively in **Figure 4**). The effect of the attenuation length is minor, and notably, a value of around 5-10nm could not fit the data in both series of samples. A 50 nm value fits well and would be in agreement with the equilibrium measurements of the spin diffusion length from the literature (particularly if the sample is slightly heated by the laser, which might reduce the spin diffusion length [43]) but the fit is not very sensitive to this value, since we have only data points up to 16 nm. Interestingly, we are able to confirm that, the reduction in THz signal does not depend on whether the THz has to go through the Cu film or not to reach the detector, by flipping the sample and measuring the emission through the opposite side (blue points in **Figure 4**). This experiment further confirms that the dominant reduction mechanism in the emission is due to the whole full multilayer's THz response, including the multiple reflections. The small difference between the measured signals obtained for both type of samples for t=16 nm could be attributed to experimental errors (slight drifts in power, alignment or sample inhomogeneities), to subtleties in the demagnetization and spin current generation (other factors than the absorption of the ferromagnet may play a role) and/or to the interfaces interfering in the spin transport [20] among other things. It is therefore difficult to accurately extract a spin current attenuation length without detailed knowledge of all these subtle effects.

We note that spin-to-charge conversion in the presence of Cu [46] and other light metals [46,47] has been recently reported. The interpretation of these observations is still not clear, but may be attributed to interface intermixing [46]. However, the reported emissions remain modest (~20% at best) in comparison to the classical heavy metal converters. Therefore, in our data, even if spin conversion within the Cu was present, it could only explain part of the signal of the Co/Cu(16 nm)/Pt sample. The rest of the signal would still require considerable spin transport across the Cu and conversion in the Pt film, resulting in a similar estimation of the spin current attenuation length.

We now discuss the possible origin on the experimental estimation of short spin diffusion lengths by Seifert et al. [18].

There, a very similar experimental procedure to ours was followed where Cu was grown either on top or in between the FM and HM layers, and were the total Cu thickness was kept constant to avoid changes in the overall THz conductivity. However, we believe it is very likely that the Cu film on top was oxidized. Uncapped Cu reacts spontaneously in ambient conditions [44,45] and creates a >2 nm oxide layer, which can be even further oxidized by time and/or heating (ex. by continuous laser pulses). If any oxidation was present in their film, the total Cu thickness and total THz conductivity would not have been conserved, and therefore the changes in THz emission efficiency should have been considered before extracting any pure spin transport property.

In conclusion, we have demonstrated that the addition of a Cu film in a spintronic emitter will lead to an almost equal reduction in THz signal despite its position within the stack. We use a transfer matrix model to fit our data and extract a spin-current attenuation length of optically excited electrons in Cu of around 50 nm. This value is in closer agreement to values of the spin diffusion length from the literature, with respect to previous estimation from THz emission [15,18]. We therefore conclude that most of the changes in THz emission are due to changes in the THz multiple reflections within the spintronic emitter and not due to spin transport. However, because the thickening of the metal film drastically changes the optical properties, only data points at thicknesses much shorter than the actual spin current attenuation length can be measured, rendering the fitting procedure prone to errors. In order to be able to extract a proper spin current attenuation length one should have extreme confidence in both the amplitude of the generated spin current and the THz optical calculation, and an excellent signal-to-noise ratio to be able to measure thick samples, which renders this method quite challenging in practice.

References

[1] V. P. Zhukov, E. V. Chulkov, and P. M. Echenique, Phys. Rev. B **73**, 1 (2006).

[2] M. Battiato, K. Carva, and P. M. Oppeneer, Phys. Rev. Lett. **105**, 027203 (2010).

[3] A. Melnikov, I. Razdolski, T. O. Wehling, *et al.*, Phys. Rev. Lett. **107**, 076601 (2011).

[4] G.-M. Choi, B.-C. Min, K.-J. Lee, *et al.*, Nat. Commun. **5**, 4334 (2014).

[5] G. Malinowski, F. Dalla Longa, J. H. H. Rietjens, *et al.*, Nat. Phys. **4**, 855 (2008).

[6] A. J. Schellekens, K. C. Kuiper, R. R. J. C. de Wit, *et al.*, Nat. Commun. **5**, 1 (2014).

[7] I. Razdolski, A. Alekhin, N. Ilin, *et al.*, Nat. Commun. **8**, 15007 (2017).

[8] M. L. M. Lalieu, P. L. J. Helgers, and B. Koopmans, Phys. Rev. B **96**, 1 (2017).

[9] S. Iihama, Y. Xu, M. Deb, *et al.*, Adv. Mater. **30**, 1804004 (2018).

[10] Q. Remy, J. Igarashi, S. Iihama, *et al.*, Adv. Sci. **7**, 2001996 (2020).

[11] J. Igarashi, Q. Remy, S. Iihama, *et al.*, Nano Lett. **20**, 8654 (2020).

[12] T. Kampfrath, M. Battiato, P. Maldonado, *et al.*, Nat. Nanotechnol. **8**, 256 (2013).

[13] T. Seifert, S. Jaiswal, U. Martens, *et al.*, Nat. Photonics **10**, 483 (2016).

[14] Y. Wu, M. Elyasi, X. Qiu, *et al.*, Adv. Mater. **29**, 1603031 (2017).

[15] G. Li, R. V. Mikhaylovskiy, K. A. Grishunin, *et al.*, J. Phys. D. Appl. Phys. **51**, 134001 (2018).

[16] C. Bull, S. M. Hewett, R. Ji, *et al.*, APL Mater. **9**, 090701 (2021).

[17] E. Saitoh, M. Ueda, H. Miyajima, *et al.*, Appl. Phys. Lett. **88**, 15 (2006).

[18] T. S. Seifert, N. M. Tran, O. Gueckstock, *et al.*, J. Phys. D. Appl. Phys. **51**, 364003 (2018).

[19] M. Meinert, B. Gliniors, O. Gueckstock, *et al.*, Phys. Rev. Appl. **14**, 1 (2020).

[20] J. Hawecker, T. Dang, E. Rongione, *et al.*, Adv. Opt. Mater. **9**, 2100412 (2021).

[21] M. B. Jungfleisch, Q. Zhang, W. Zhang, *et al.*, Phys. Rev. Lett. **120**, 207207 (2018).

[22] J. Bass and W. P. Pratt, J. Phys. Condens. Matter **19**, 183201 (2007).

[23] A. J. Schellekens, N. de Vries, J. Lucassen, *et al.*, Phys. Rev. B **90**, 104429 (2014).

[24] R. B. Wilson, Y. Yang, J. Gorchon, *et al.*, Phys. Rev. B **96**, 045105 (2017).

[25] A. L. Chekhov, Y. Behovits, J. J. F. Heitz, *et al.*, Phys. Rev. X **11**, 41055 (2021).

[26] M. Bauer, A. Marienfeld, and M. Aeschlimann, Prog. Surf. Sci. **90**, 319 (2015).

[27] B. Ferguson and X. Zhang, Nat. Mater. **1**, 26 (2002).

[28] M. Tonouchi, Nat. Photonics **1**, 97 (2007).

[29] Y. Yang, S. Dal Forno, and M. Battiato, Phys. Rev. B **104**, 1 (2021).

[30] E. M. Purcell, Phys. Rev. **69**, 674 (1946).

[31] Q. Lu, X. Chen, C.-L. Zou, *et al.*, Opt. Express **26**, 30851 (2018).

[32] J. Bravo-Abad and M. Soljačić, Springer Ser. Opt. Sci. **170**, 325 (2012).

[33] C. Sauvan, J. P. Hugonin, I. S. Maksymov, *et al.*, Phys. Rev. Lett. **110**, 1 (2013).

[34] B. Romeira and A. Fiore, IEEE J. Quantum Electron. **54**, (2018).

[35] (n.d.).

[36] T. F. Heinz, Nonlinear Optics of Surfaces and Adsorbates, 1982.

[37] S. Khorasani and B. Rashidian, J. Opt. A Pure Appl. Opt. **4**, 251 (2002).

[38] H. Selig, M. Khazan, and I. Wilke, in *Conf. Dig. 2000 Conf. Lasers Electro-Optics Eur.* (IEEE, 2000), p. 1.

[39] F. Sanjuan and J. O. Tocho, in *Lat. Am. Opt. Photonics Conf.* (OSA, Washington, D.C., 2012), p. LT4C.1.

[40] H. Yasuda, Proc. 2008 Asia Pacific Microw. Conf. APMC 2008 1 (2008).
[41] M. A. Ordal, R. J. Bell, R. W. Alexander, *et al.*, Appl. Opt. **24**, 4493 (1985).
[42] Hagemann H.-J., G. W., and K. C., **DESY-repor**, (1974).
[43] S. Yakata, Y. Ando, T. Miyazaki, *et al.*, Jpn. J. Appl. Phys. **45**, 3892 (2006).
[44] P. Keil, D. Lützenkirchen-Hecht, and R. Frahm, AIP Conf. Proc. **882**, 490 (2007).
[45] J. J. Díaz León, D. M. Fryauf, R. D. Cormia, *et al.*, in *Low-Dimensional Mater. Devices 2016*, edited by N. P. Kobayashi *et al.* (2016), p. 99240O.
[46] O. Gueckstock, L. Nádvorník, M. Gradhand, *et al.*, Adv. Mater. **33**, 2006281 (2021).
[47] H. Zhang, Z. Feng, J. Zhang, *et al.*, Phys. Rev. B **102**, 024435 (2020).

Acknowledgments

This work was supported by the ANR projects ANR-20-CE24-0003 SPOTZ and ANR-20-CE09-0013 UFO, by the impact project LUE-N4S part of the French PIA project "Lorraine Université d'Excellence", reference ANR-15IDEX-04-LUE, by the Région Grand Est and the Metropole Grand Nancy, for the Chaire PLUS and the "FEDER-FSE Lorraine et Massif Vosges 2014-2020", a European Union Program.

Competing financial interests

The authors declare no competing financial interests**.**